

**Positron Emission Tomography**

# CycloSiFA: The Next Generation of Silicon-Based Fluoride Acceptors for Positron Emission Tomography (PET)

Matthias Mawick, Carolin Jaworski, Jens Bittermann, Ljuba Iovkova, Yinglan Pu, Carmen Wängler, Björn Wängler, Klaus Jurkschat,\* Norbert Krause,\* and Ralf Schirrmacher\*

Dedicated to Professor Manfred T. Reetz on the occasion of his 80<sup>th</sup> birthday

**Abstract:** The ring-opening Si-fluorination of a variety of azasilole derivatives *cyclo*-1-(*i*Pr<sub>2</sub>Si)-4-X-C<sub>6</sub>H<sub>3</sub>-2-CH<sub>2</sub>NR (**4**: R=2,6-*i*Pr<sub>2</sub>C<sub>6</sub>H<sub>3</sub>, X=H; **4a**: R=2,4,6-Me<sub>3</sub>C<sub>6</sub>H<sub>2</sub>, X=H; **9**: R=2,6-*i*Pr<sub>2</sub>C<sub>6</sub>H<sub>3</sub>, X=*t*BuMe<sub>2</sub>SiO; **10**: R=2,6-*i*Pr<sub>2</sub>C<sub>6</sub>H<sub>3</sub>, X=OH; **13**: R=2,6-*i*Pr<sub>2</sub>C<sub>6</sub>H<sub>3</sub>, X=HCCCCH<sub>2</sub>O; **22**: R=2,6-*i*Pr<sub>2</sub>C<sub>6</sub>H<sub>3</sub>, X=*t*BuMe<sub>2</sub>SiCH<sub>2</sub>O) with different <sup>19</sup>F-fluoride sources was studied, optimized and the experience gained was used in a translational approach to create a straightforward <sup>18</sup>F-labelling protocol for the azasilole derivatives [<sup>18</sup>F]**6** and [<sup>18</sup>F]**14**. The latter constitutes a potential clickable *CycloSiFA* prosthetic group which might be used in PET tracer development using Cu-catalysed triazole formation. Based on our findings, *CycloSiFA* has the potential to become a new entry into non-canonical labelling methodologies for radioactive PET tracer development.

## Introduction

The advent of non-canonical radio-fluorine (fluorine-18 isotope, <sup>18</sup>F, half-life = 109.7 min) labelling chemistries based on silicon-, boron-, aluminium-<sup>18</sup>F formation and the most recently reported aryl fluorosulfate (SuFEx) click radiolabelling has introduced new synthetic tools to radiopharmaceutical chemistry. It facilitated the development of molecular imaging agents for Positron Emission Tomography (PET).<sup>[1–6]</sup>

PET is a diagnostic imaging modality based on the detection of gamma rays originating from positron electron annihilation.<sup>[7,8]</sup> The positron is the decay product of positron emitting radioisotopes (e.g. <sup>18</sup>F). To obtain clinically useful radiotracers for in vivo imaging the <sup>18</sup>F-isotope has to be stably bound to the imaging agent. Since radiochemists have to combat the radioactive decay, the introduction of <sup>18</sup>F has to be swift and the workup procedures streamlined. <sup>18</sup>F-PET tracer development has previously been limited mostly to carbon-<sup>18</sup>F bond chemistry,<sup>[9,10]</sup> characterized by the use of high temperatures, side product formation and sometimes long reaction times. Structurally complex molecules (peptides and proteins) could only be labelled by synthesizing small <sup>18</sup>F-labelled prosthetic groups subsequently being attached to the complex molecules.<sup>[11]</sup> Complex radiochemistry and laborious work up procedures hindered the dissemination of structurally intricate <sup>18</sup>F-imaging agents.

Shifting away from the classical <sup>18</sup>F-carbon bond radiochemistry, alternative elements such as boron,<sup>[12]</sup> aluminium,<sup>[13]</sup> silicon and most recently sulphur,<sup>[14]</sup> all forming strong chemical bonds with fluorine, were employed to bind the <sup>18</sup>F-isotope in one single step to complex molecules bearing a multitude of unprotected chemical groups. These one-step <sup>18</sup>F-labelling protocols constitute a technical improvement over a multistep synthetic approach. The boron- and silicon <sup>18</sup>F-chemistries additionally demonstrated that high molar activities A<sub>m</sub> (radioactivity/mol radiotracer) can be reached by isotopic exchange (IE) reactions where a non-radioactive fluorine (<sup>19</sup>F isotope), connected to a boron or silicon atom, is simply replaced by radioactive <sup>18</sup>F. The most recently introduced SuFEx labelling approach confirmed these findings. The amount of precursor (fluoroborates, fluorosilicates and fluorosulfates) can be reduced to nano-molar quantities, a prerequisite to achieve high A<sub>m</sub> formerly not possible in IE carbon-<sup>18</sup>F chemistry. Aluminium-<sup>18</sup>F chemistry capitalizes

[\*] M. Mawick, J. Bittermann, Dr. L. Iovkova, Prof. Dr. N. Krause  
Fakultät für Chemie und Chemische Biologie, Lehrstuhl für  
Organische Chemie, Technische Universität Dortmund  
Otto-Hahn-Straße 6, 44227 Dortmund (Germany)  
E-mail: norbert.krause@tu-dortmund.de

C. Jaworski, Y. Pu, Prof. Dr. R. Schirrmacher  
Department of Oncology, Division of Oncological Imaging, University of Alberta  
Edmonton, AB T6G 1Z2 (Canada)  
E-mail: schirrma@ualberta.ca

Prof. Dr. C. Wängler, Prof. Dr. B. Wängler  
Department of Clinical Radiology and Nuclear Medicine, Medical Faculty Mannheim of Heidelberg University  
Theodor-Kutzer-Ufer 1-3, 68167 Mannheim (Germany)

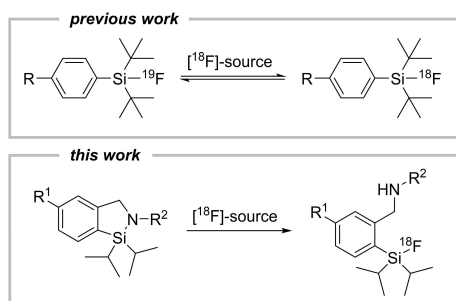
Prof. Dr. K. Jurkschat  
Fakultät für Chemie und Chemische Biologie, Technische Universität Dortmund  
Otto-Hahn-Straße 6, 44227 Dortmund (Germany)  
E-mail: klaus.jurkschat@tu-dortmund.de

© 2023 The Authors. *Angewandte Chemie International Edition* published by Wiley-VCH GmbH. This is an open access article under the terms of the Creative Commons Attribution Non-Commercial NoDerivs License, which permits use and distribution in any medium, provided the original work is properly cited, the use is non-commercial and no modifications or adaptations are made.

on a different labelling Scheme by preforming [Al–F] aqua complexes which can be further react with radiometal chelators.<sup>[15]</sup>

The Al-, B-, and Si-based <sup>18</sup>F-radiochemistries have proven their clinical applicability and became already valuable additions to the portfolio of available radiotracers for PET imaging of neuroendocrine tumours,<sup>[16–20]</sup> prostate specific membrane antigen (PSMA)<sup>[21]</sup> and metastatic lung cancer.<sup>[22a]</sup> Previously disclosed silicon fluoride acceptors (SiFAs)<sup>[2a]</sup> can be considered being the first generation of Si-based <sup>18</sup>F-radiopharmaceuticals (Scheme 1). [<sup>18</sup>F]SiTATE labelling has been clinically consolidated in more than 3000 cancer patients (several clinics in Germany) for the diagnosis of neuro-endocrine tumours and most recently for meningioma imaging.<sup>[22b]</sup>

SiFAs are limited to IE reactions because any other group than F e.g. Cl, Br or I connected to the Si centre yields a chemically unstable precursor compound that cannot be further processed or derivatized for <sup>18</sup>F-radio-labelling. Although the SiFA chemistry yields relatively high A<sub>m</sub> via IE, a direct labelling approach based on leaving group substitution might be advantageous by circumventing limitations imposed by the IE equilibrium to reach highest radiochemical conversions. To extend the field of Si-based fluorination chemistry and to devise an alternative leaving-group based <sup>18</sup>F-labelling protocol, herein we introduce *CycloSiFA*, the first in kind cyclic labelling precursor amenable towards <sup>18</sup>F-radiofluorination via Si–N ring opening reaction. *CycloSiFA* like the original SiFA can only be used for the <sup>18</sup>F-labeling of large organic molecules such as peptides and proteins. The change of lipophilicity, by introducing SiFA, for small biomolecules would be too drastic and negatively impact the tracer's biodistribution. The calculated logP value of *CycloSiFA* of 7.3 stipulates the addition of hydrophilic auxiliaries (e.g. aspartic acids) to the biomolecule to be labelled to reduce the compound's overall lipophilicity, a crucial parameter for successful PET probe development. This strategy has been proven applicable to previously labelled SiFA compounds such a [<sup>18</sup>F]SiTATE, a compound for clinical somatostatin receptor imaging in cancer patients.<sup>[19]</sup>



**Scheme 1.** <sup>18</sup>F-radiolabelling reactions using isotope exchange equilibrium with [<sup>18</sup>F]SiFAs or ring opening reaction of *CycloSiFAs*.

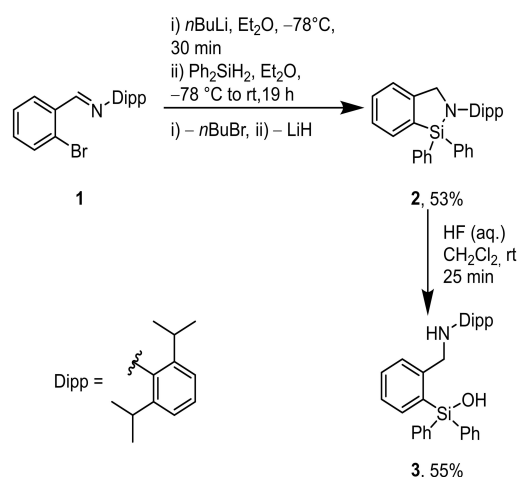
## Results and Discussion

The literature-known model compound 2-(2,6-diisopropylphenyl)-1,1-diphenyl-2,3-dihydro-1*H*-benzo[*c*][1,2]azasilole, **2**, was synthesized according to Jambor et al. via halogen-metal exchange between *o*-bromobenzylidiphenylphenyl imine, *o*-BrC<sub>6</sub>H<sub>4</sub>C(H)NC<sub>6</sub>H<sub>3</sub>-[CH(CH<sub>3</sub>)<sub>2</sub>]<sub>2</sub>-2,5, **1**, and *n*-butyl lithium, *n*BuLi, followed by substitution with diphenylsilane, Ph<sub>2</sub>SiH<sub>2</sub> (Scheme 2). The formation of the Si–N bond is the result of spontaneous hydrosilylation of the CH=N imine moiety.<sup>[23]</sup>

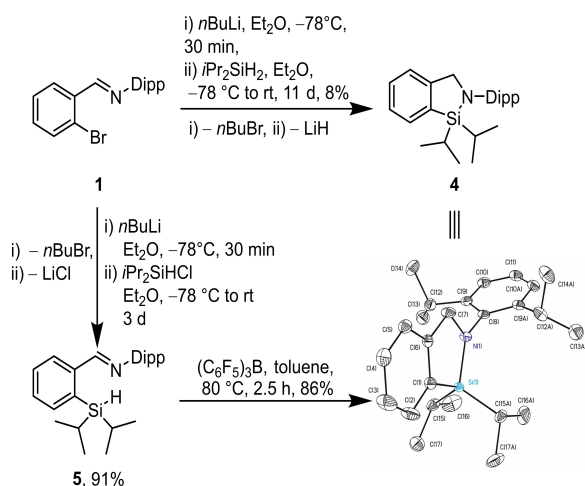
Attempts to obtain the desired SiFA compound by treatment of **2** with potassium fluoride gave no conversion, whereas reaction with tetrabutylammonium fluoride, *n*Bu<sub>4</sub>NF, hereafter referred to as TBAF, gave a complex reaction mixture which was not further analysed. Likewise, ring opening of the cyclic compound using commercial conc. hydrofluoric acid (48–51 %) afforded no fluorinated product. Rather, the silanol **3** was isolated, indicating a low hydrolytic stability of the Si–F bond as previously reported by Ametamey et al. for similar compounds.<sup>[24]</sup> In order to improve the hydrolytic stability, sterically more demanding groups needed to be attached to the silicon atom.

Classical SiFA compounds use *tert*-butyl substituents to shield the Si–F bonds from hydrolytic degradation. The use of di-*tert*-butylsilane in the reaction shown above gave no substitution product, as did the application of Ir-catalysts for C–H-bond-activation,<sup>[25a]</sup> the use of directed *ortho*-metalation or a synthesis pathway via protected amines.

Since fluorodiisopropylphenylsilanes bearing a methyl group in *ortho*-position to the silicon substituent were reported to have good hydrolytic stability (half-life 302 h), diisopropylsilane was chosen as the reactant to afford the sterically more demanding *CycloSiFA* compound **4**.<sup>[24]</sup> The transformation of **1** with *n*BuLi and *i*Pr<sub>2</sub>SiH<sub>2</sub>, however, gave 2-(2,6-diisopropylphenyl)-1,1-diisopropyl-2,3-dihydro-1*H*-benzo[*c*][1,2]azasilole, **4**, with a poor yield of 8 % after 11 d reaction time (Scheme 3).



**Scheme 2.** Synthesis of 2-(2,6-diisopropylphenyl)-1,1-diphenyl-2,3-dihydro-1*H*-benzo[*c*][1,2]azasilole **2** and its reaction with hydrogen fluoride, HF. Commercial aqueous HF with concentration of 48–51 % was used.



**Scheme 3.** Optimized synthesis and molecular structure of 2-(2,6-diisopropylphenyl)-1,1-diisopropyl-2,3-dihydro-1*H*-benzo[*c*][1,2]azasilole **4** (*CycloSiFA*).

The use of THF instead of diethyl ether did not accelerate the reaction. To optimize the yield, the reaction was divided into two separate steps. First, the lithiation was conducted using *n*BuLi and diisopropylchlorosilane to afford the intermediate silane **5** in 91 % yield. Then, the use of the strong Lewis acid B(C<sub>6</sub>F<sub>5</sub>)<sub>3</sub> enabled cyclization to *CycloSiFA* **4** in 86 % yield. Structure verification was accomplished by single crystal X-ray diffraction analysis<sup>[25b]</sup> (for details see the Supporting Information). *CycloSiFA* **4** shows excellent stability at room temperature, even in solution. However, due to its acid sensitivity, purification by column chromatography needed to be performed with neutral or basic aluminium oxide to prevent ring opening to the corresponding silanol. *CycloSiFAs* with different substituents at the nitrogen atom were prepared in lower yields by this route but they showed lower hydrolytic stability.<sup>[26]</sup>

The optimization for the <sup>19</sup>F-fluorination of *CycloSiFA* **4** giving *SiFA* **6** was performed at room temperature in CH<sub>2</sub>Cl<sub>2</sub>. The use of 2.0 molar equivalents of conc. hydrofluoric acid or HF·py showed quantitative conversion to the desired product after just 10 min (Table 1, entries 1, 2).

In the case of radiofluorination with <sup>18</sup>F, this would imply a quantitative formation of the radiotracer, while classical *SiFA* compounds can only reach a theoretic maximum of 67 % due to the isotopic exchange equilibrium. Triethylamine trihydrofluoride (3.0 equiv) required a longer reaction time of 2 h to give a good yield of 95 % (entry 3). Boron trifluoride diethyl etherate (4.0 equiv) at 30 °C was also able to convert the substrate in quantitative yield after 2 h (entry 4).

Even after sonication and prolonged reaction times, the use of TBAF without an additive or with acetic acid did not yield any product (entries 6, 7). The addition of oxalic acid enabled product formation with 66 % yield after 90 min (entry 5). Such reaction conditions are known to increase the reactivity and are also applied in the radiofluorination with <sup>18</sup>F.<sup>[19,20]</sup>

During this optimization study, potassium fluoride and kryptofix 222 did not generate the fluorinated product **6**. The addition of weak diluted acids or glacial acetic acid did not change the outcome (entries 8–11). The optimization showed that fluorination of *CycloSiFA* model compound **4** could be achieved not only using HF-containing reagents but also classical radiochemical labelling conditions. Moreover, unlike the diphenyl derivative **2**, the stability of **4** against TBAF in the presence of water enables the synthesis of substituted *CycloSiFAs* for use in imaging applications.

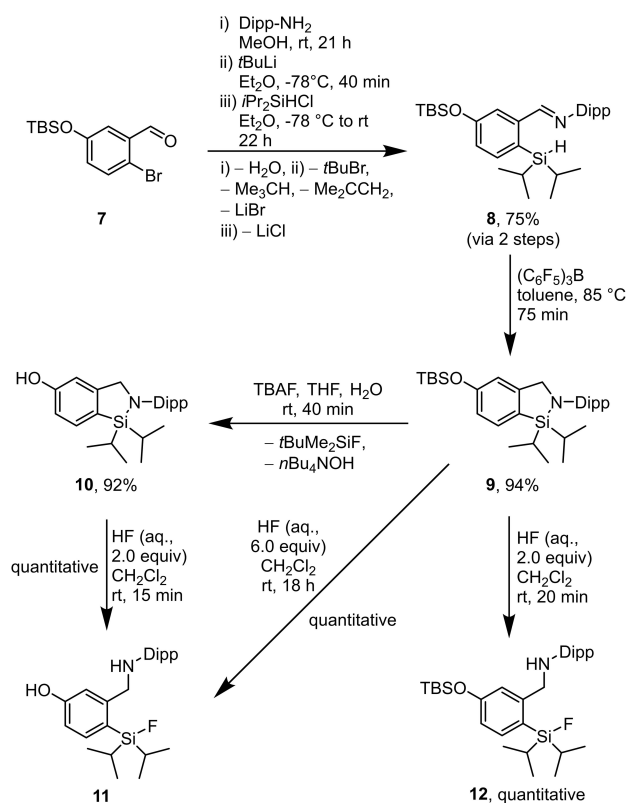
The synthesis of the phenolic *CycloSiFA* derivative **10** was performed starting with the imine formation by condensation of the known aldehyde **7**<sup>[27]</sup> and 2,6-diisopropylphenyl amine (Dipp-amine, Scheme 4).

The subsequent halogen-metal exchange was performed using *t*BuLi instead of *n*BuLi since the reaction proceeded

**Table 1:** Optimization of the fluorination of *CycloSiFA* compound **4**.<sup>[a]</sup>

Entry	[ <sup>19</sup> F <sup>-</sup> ]-Source	Estimated concentration	Additive	t	Yield [%] <sup>[b]</sup>
1	HF (aq., 2.0 equiv)	<i>c</i> (Si) ≈ 50 mM, <i>c</i> (F) ≈ 100 mM		10 min	quantitative
2	HF·py (2.0 equiv)	<i>c</i> (Si) ≈ 100 mM, <i>c</i> (F) ≈ 200 mM		10 min	quantitative
3	Et <sub>3</sub> N·3HF (3.0 equiv)	<i>c</i> (Si) ≈ 95 mM, <i>c</i> (F) ≈ 286 mM		2 h	95
4 <sup>[c]</sup>	BF <sub>3</sub> ·OEt <sub>2</sub> (4.0 equiv)	<i>c</i> (Si) ≈ 95 mM, <i>c</i> (F) ≈ 381 mM		2 h	quantitative
5 <sup>[d]</sup>	TBAF <sup>[e]</sup> (1.0 equiv)	<i>c</i> (Si) ≈ 67 mM, <i>c</i> (F) ≈ 67 mM	Oxalic acid <sup>[f]</sup>	90 min	66
6 <sup>[d]</sup>	TBAF <sup>[e]</sup> (1.0 equiv)	<i>c</i> (Si) ≈ 77 mM, <i>c</i> (F) ≈ 77 mM	Acetic acid <sup>[f]</sup>	3 h	n. c.
7 <sup>[d]</sup>	TBAF <sup>[e]</sup> (1.0 equiv)	<i>c</i> (Si) ≈ 91 mM, <i>c</i> (F) ≈ 91 mM		23 h	n. c.
8 <sup>[d]</sup>	[K <sup>+</sup> C 222] F <sup>-</sup> (2.0 equiv)	<i>c</i> (Si) ≈ 63 mM, <i>c</i> (F) ≈ 125 mM	Oxalic acid <sup>[f]</sup>	2 h	n. c.
9 <sup>[d]</sup>	[K <sup>+</sup> C 222] F <sup>-</sup> (2.0 equiv)	<i>c</i> (Si) ≈ 63 mM, <i>c</i> (F) ≈ 125 mM	Acetic acid <sup>[f]</sup>	22 h	n. c.
10 <sup>[d]</sup>	[K <sup>+</sup> C 222] F <sup>-</sup> (2.0 equiv)	<i>c</i> (Si) ≈ 98 mM, <i>c</i> (F) ≈ 196 mM	Acetic acid <sup>[g]</sup>	20 h	n. c.
11 <sup>[d]</sup>	[K <sup>+</sup> C 222] F <sup>-</sup> (1.0 equiv)	<i>c</i> (Si) ≈ 100 mM, <i>c</i> (F) ≈ 200 mM		20 h	n. c.

<sup>[a]</sup> Reactions at 22 °C in dry CH<sub>2</sub>Cl<sub>2</sub>. <sup>[b]</sup> Yield of isolated product. <sup>[c]</sup> At 30 °C. <sup>[d]</sup> Sonication for 5 min after mixing. <sup>[e]</sup> 1 M in THF. <sup>[f]</sup> 0.5 M in H<sub>2</sub>O. <sup>[g]</sup> Glacial acetic acid. n. c. = no conversion.



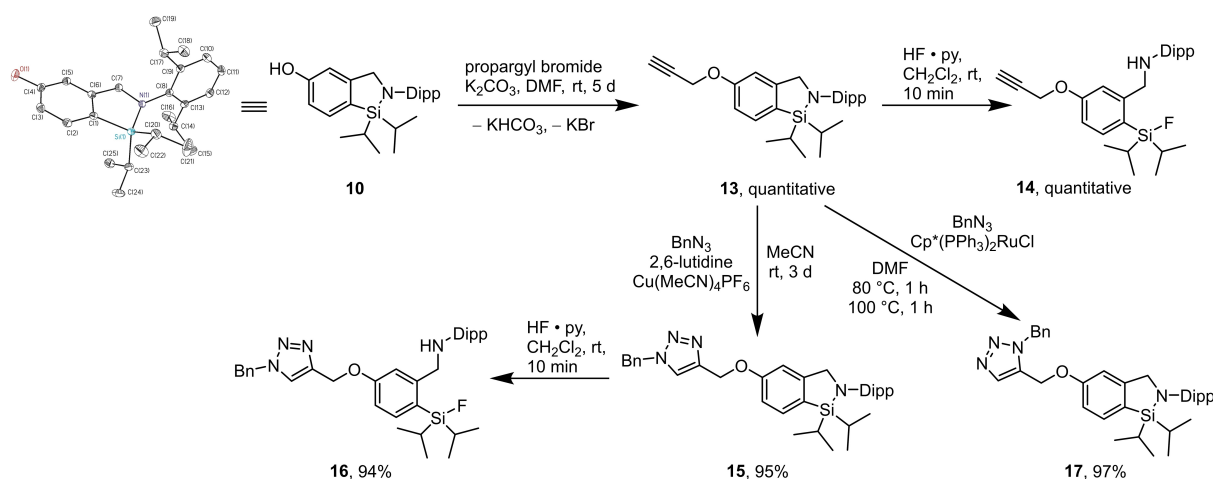
**Scheme 4.** Synthesis of the *CycloSiFA* **10** containing a hydroxy substituent at the aryl backbone and its deprotection/ring opening.

faster, and the progress of the reaction could be monitored visually because of a strong colour change to yellow and formation of a precipitate. Reaction of the lithiated imine with diisopropylchlorosilane gave the intermediate **8** in 75 % yield over two steps. Cyclization to the *tert*-butyldimethylsilyl-protected (hereafter referred to as TBS-protected) *CycloSiFA* **9** in the presence of B(C<sub>6</sub>F<sub>5</sub>)<sub>3</sub> proceeded

smoothly (94 % yield). This compound showed a unique reactivity towards different fluoride sources. The use of TBAF in THF enabled deprotection of the silyl ether to give the free phenol **10** after 40 min with 92 % yield. The Si–N bond remained intact and the overall yield from **7** to **10** was 65 % over four steps. The phenol **10** could further be converted into the opened SiFA **11** by reaction with commercial hydrofluoric acid (48–51 %). This compound could also be obtained directly from **9** in quantitative yield by treatment with 6.0 equiv. of conc. hydrofluoric acid for 18 h at room temperature. However, if **9** was reacted with only 2.0 equiv. of conc. HF for 20 min, the Si–N bond was cleaved but the silyl ether remained intact to afford **12** with quantitative yield.

The structure in the solid state (for details see the Supporting Information) of *CycloSiFA* **10** was confirmed by single crystal X-ray diffraction analysis.<sup>[25b]</sup> It shows the presence of the phenolic oxygen atom but in contrast to the structure of phenol<sup>[28a–d]</sup> no intermolecular hydrogen bond. This was verified by an infrared spectrum of a single crystalline sample of **10** showing a sharp absorption at  $\tilde{\nu}_{\text{OH}} = 3522 \text{ cm}^{-1}$ . For comparison, an IR spectrum of crystalline phenol measured on the same IR spectrometer shows a  $\tilde{\nu}_{\text{OH}}$  at  $3223 \text{ cm}^{-1}$  unambiguously indicating the presence of O–H...O hydrogen bond. Notably, instead of showing an O–H...O hydrogen bond, *CycloSiFA* **10** forms a centrosymmetric head-to-tail dimer via a weak H1...centre C11 A/C12 A interaction at a distance of 2.543(1) Å. Most remarkably, there is a O1...O1B interaction at a distance of 2.870(1) Å being shorter than twice the van der Waals radius<sup>[29a]</sup> of oxygen (1.52 Å). This situation resembles the unusual F...F interactions recently reported for {(F<sub>3</sub>C)<sub>3</sub>CO<sub>3</sub>SiH} which were interpreted as originating from London dispersion forces.<sup>[29b]</sup>

The next step was the preparation of alkynyl-substituted *CycloSiFA* **13** from the corresponding hydroxyl-substituted derivative **10** and propargyl bromide via nucleophilic substitution (Scheme 5). The desired propargyl ether was



**Scheme 5.** Synthesis of the triazoles **15** and **17** by the reaction of the propargyl ether **13** with benzyl azide, BnN<sub>3</sub>, catalysed by tetraacetonitrile copper hexafluorophosphate, [Cu(MeCN)<sub>4</sub>]PF<sub>6</sub>, and pentamethylcyclopentadienyl bis(triphenylphosphane) ruthenium chloride, [Cp\*(PPh<sub>3</sub>)<sub>2</sub>Ru]Cl, respectively (CuAAC- and RuAAC-type reactions).

isolated in quantitative yield and fluorinated to afford SiFA compound **14**. The alkyne **13** can easily be linked to other biomolecules to afford radiotracer precursors by click reaction.<sup>[30]</sup> Copper- and ruthenium-catalysed azide-alkyne cycloadditions (CuAAC and RuAAC) are amongst the widely used click reactions that allow the formation of biologically stable 1,2,3-triazoles. Thus, as a test reaction, CuAAC between the alkyne derivative **13** and benzyl azide afforded the 1,4-disubstituted 1,2,3-triazole **15** in excellent yield of 95%. Fluorination of the reaction product gave the SiFA-fluoride **16** in very good yield (94%). Similar, RuAAC of **13** with benzyl azide afforded the 1,5-disubstituted 1,2,3-triazole **17** in excellent yield of 97%. The substitution patterns of both cycloaddition products were determined using <sup>1</sup>H–<sup>15</sup>N-HMBC NMR experiments. The successful realization of both click reaction conditions together with the stability of the *CycloSiFAs* should enable the formation of on-demand libraries of various radiotracers. Moreover, differently substituted *CycloSiFAs* could be synthesized for different applications, such as azides, maleimides, amines, aldehydes or tetrazines. To enhance the solubility of the cyclic derivatives in aqueous media for in vivo use, one could add water soluble linkers.<sup>[20]</sup>

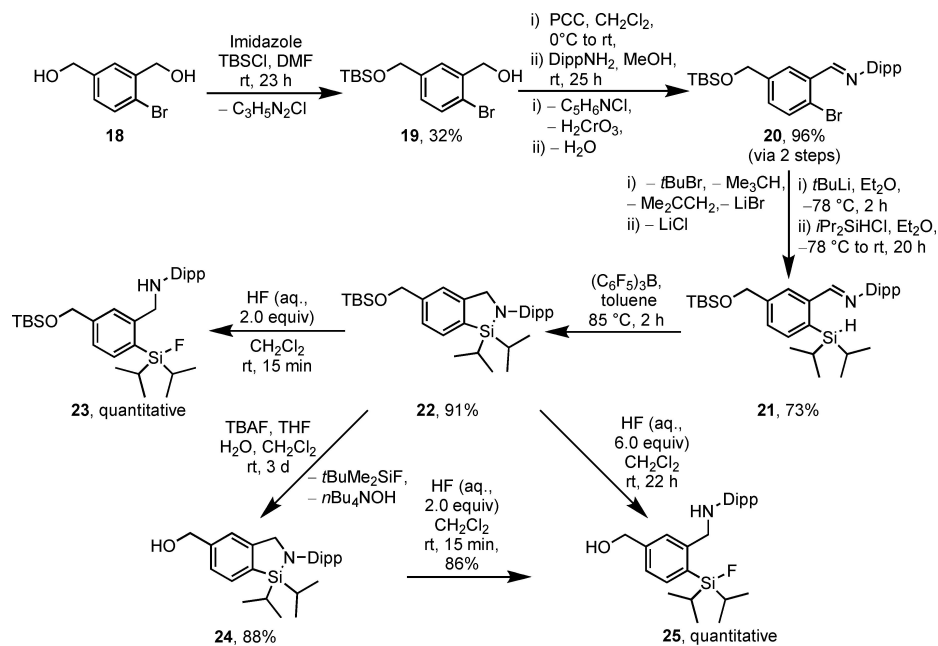
To broaden the library of possible *CycloSiFA* compounds, the *CycloSiFA* derivative **24** bearing a hydroxymethyl substituent was prepared in a similar manner as the hydroxy-substituted compound **10** (Scheme 6).

Starting with the diol **18**,<sup>[31]</sup> a statistical TBS-protection of a single hydroxy group was performed to give the silyl ether **19** in 32% yield.<sup>[32]</sup> Oxidation of the unprotected alcohol with pyridinium chlorochromate (PCC) and subsequent condensation of the aldehyde with Dipp-amine afforded the imine **20** in 96% yield over two steps. Halogen-lithium exchange and substitution with *i*Pr<sub>2</sub>SiHCl gave the

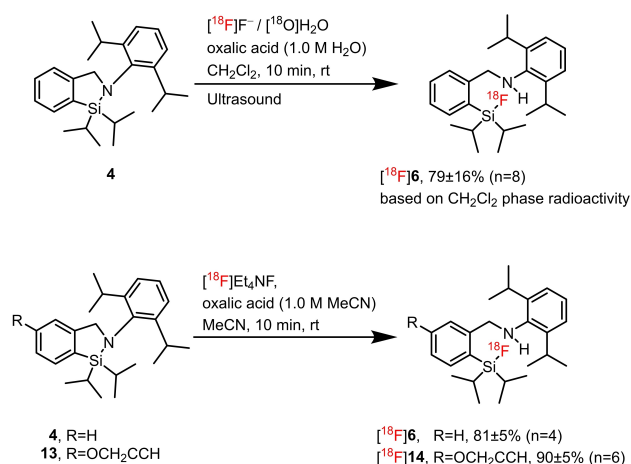
silane **21** in 73% yield. After cyclisation to the TBS-protected *CycloSiFA* **22** in the presence of (C<sub>6</sub>F<sub>5</sub>)<sub>3</sub>B (91% yield), the same reactivity pattern in deprotection/fluorination reactions was observed as for the silyl ether **9**. With 2.0 molar equiv. of conc. hydrofluoric acid, complete cleavage of the Si–N-bond was observed after a reaction time of 15 min to give compound **23** in quantitative yield. With 6.0 molar equiv. of conc. hydrofluoric acid, additional cleavage of the silyl ether was achieved after 22 h reaction time to give the benzyl alcohol **25**. Simple deprotection of the TBS-ether **22** with TBAF in THF proceeded much slower compared to phenol **9**, yielding the desired *CycloSiFA* **24** in 88% yield after a reaction time of 3 d at room temperature. In the presence of conc. HF, **24** undergoes facile ring opening to afford **25** (86% yield). The overall yield for the synthesis of compound **24** starting from TBS-protected alcohol **19** was 56% over five steps.

The first <sup>18</sup>F-labelling approach of *CycloSiFA* revolved around our established “cold” non-radioactive fluorination protocol, employing aqueous <sup>18</sup>F<sup>−</sup> and the labelling precursors **4** dissolved in CH<sub>2</sub>Cl<sub>2</sub> to yield [<sup>18</sup>F]**6**. From previous experiments, the “cold” fluorinations of **4** resulting in the formation of **6** were performed in a non-mixable liquid-liquid two-phase system consistent of **4** dissolved in CH<sub>2</sub>Cl<sub>2</sub> and the <sup>18</sup>F<sup>−</sup> source provided as an aqueous solution of <sup>18</sup>F<sup>−</sup> in <sup>18</sup>O-enriched water (Scheme 7).

The [<sup>18</sup>O]H<sub>2</sub>O is used in the cyclotron production of the <sup>18</sup>F isotope where an <sup>18</sup>O isotope is converted in a (p, n) nuclear reaction into an <sup>18</sup>F isotope. The theoretical molar activity of <sup>18</sup>F (A<sub>m</sub>, defined as the <sup>18</sup>F radioactivity amount divided by the total molarity of <sup>18</sup>F and <sup>19</sup>F impurities) is 63 TBq/μmol and cannot be reached in practice.<sup>[33–40]</sup> Non-radioactive <sup>19</sup>F, inevitably diluting <sup>18</sup>F, mostly stems from the tubing material used to move the <sup>18</sup>F solution from the



**Scheme 6.** Synthesis of *CycloSiFA* **24** containing a hydroxymethyl substituent and deprotection/ring opening.



**Scheme 7.** Upper row: Radiochemical fluorination of **4** to  $[^{18}\text{F}]\text{6}$  using ultrasound (100  $\mu\text{L}$   $\text{CH}_2\text{Cl}_2$  + 40  $\mu\text{L}$   $\text{H}_2\text{O}$ ). Only 1–2% of  $^{18}\text{F}^-$  were transferred from the  $[^{18}\text{O}]\text{H}_2\text{O}$  phase into the  $\text{CH}_2\text{Cl}_2$  phase. Thin layer chromatography (TLC) evaluation of the  $\text{CH}_2\text{Cl}_2$  layer revealed a radiochemical conversion (RCC) of  $^{18}\text{F}^-$  into  $[^{18}\text{F}]\text{6}$  of 79±16% (based on only 1–2% of  $^{18}\text{F}^-$  being transferred to the  $\text{CH}_2\text{Cl}_2$  phase). Bottom row: Radiofluorination of **4** and **13** in acetonitrile yielding  $[^{18}\text{F}]\text{6}$  and  $[^{18}\text{F}]\text{14}$  in RCC of 81±5% and 90±5%, respectively. The RCC in all cases was determined by radio-TLC.

cyclotron target chamber to the automated synthesis unit for further processing. Consequently, the  $A_m$  of  $^{18}\text{F}$  is found to much lower being in the range of 22–9900 GBq/ $\mu\text{mol}$  with one report referring to a measured  $A_m$  of 43 TBq/ $\mu\text{mol}$  at the end of bombardment. In our labelling scenario we only used radioactivity amounts in the range of 300–500 MBq following the ALARA principle to reduce radiation exposure in our manual labelling setup.

Oxalic acid was added to the  $[^{18}\text{O}]\text{H}_2\text{O}$  phase before sonication to lower the pH of the  $[^{18}\text{O}]\text{H}_2\text{O}$  from 4.4 to 1.4 as it was found that no radiochemical conversion, hereafter

referred to RCC, was observed at a pH of 4.4. To optimize  $^{18}\text{F}$ -fluorination using sonication, we had to establish the optimal depth of immersion of the reaction vial into the ultrasound bath to increase liquid-liquid phase interference for efficient radioactivity exchange between the two liquid phases. This process proved to be labour intensive and yielded only low  $^{18}\text{F}$ -transfer rates. The influence of using different volumes of  $^{18}\text{F}^-/\text{H}_2\text{O}$  and  $\text{CH}_2\text{Cl}_2$  on the RCC yielding  $[^{18}\text{F}]\text{6}$  were investigated. Extensive evaluation revealed that even under optimized conditions (cf. experimental part), only 1–2% of the  $^{18}\text{F}$ -radioactivity from the aqueous  $[^{18}\text{O}]\text{H}_2\text{O}$  phase was transported into the  $\text{CH}_2\text{Cl}_2$  layer. Analysis of the  $\text{CH}_2\text{Cl}_2$  radioactivity content using radio-thin layer chromatography (TLC) revealed that only 79±18% of the radioactivity present in the  $\text{CH}_2\text{Cl}_2$  phase accounted for  $[^{18}\text{F}]\text{6}$  (n=8). The rest radioactivity was identified by TLC being unreacted  $^{18}\text{F}^-$ . Neither increasing the concentration of **4** nor adding a phase transfer catalyst such as K222 to the aqueous and  $\text{CH}_2\text{Cl}_2$  phases improved the  $^{18}\text{F}$ -transfer rate or the RCC. The technical difficulties encountered (e.g. finding the optimal depth of immersion) and the low efficiency of  $^{18}\text{F}$ -transfer between the two phases rendered this labelling approach unsuitable for radiotracer development and automation.

In order to optimize  $^{18}\text{F}$ -labelling of **4** and to make the protocol more applicable to future automation, we developed a homogeneous one-phase liquid labelling method in acetonitrile. This methodology accounts for the unique conditions required for  $^{18}\text{F}$ -radiolabelling and prospective automation. The low amount of  $[^{18}\text{F}]\text{F}^-$  (M=pico- to nanomolar) used in our experiments (300–500 MBq were used) and short half-life of  $^{18}\text{F}$  ( $t_{1/2}=110$  min) necessitate the enhancement of  $^{18}\text{F}^-$  anion nucleophilicity and the ability to quickly purify the labelling reaction mixture by solid phase extraction or high performance liquid chromatography (HPLC). The introduction of a homogeneous one-phase reaction system is a common denominator in most  $^{18}\text{F}$ -

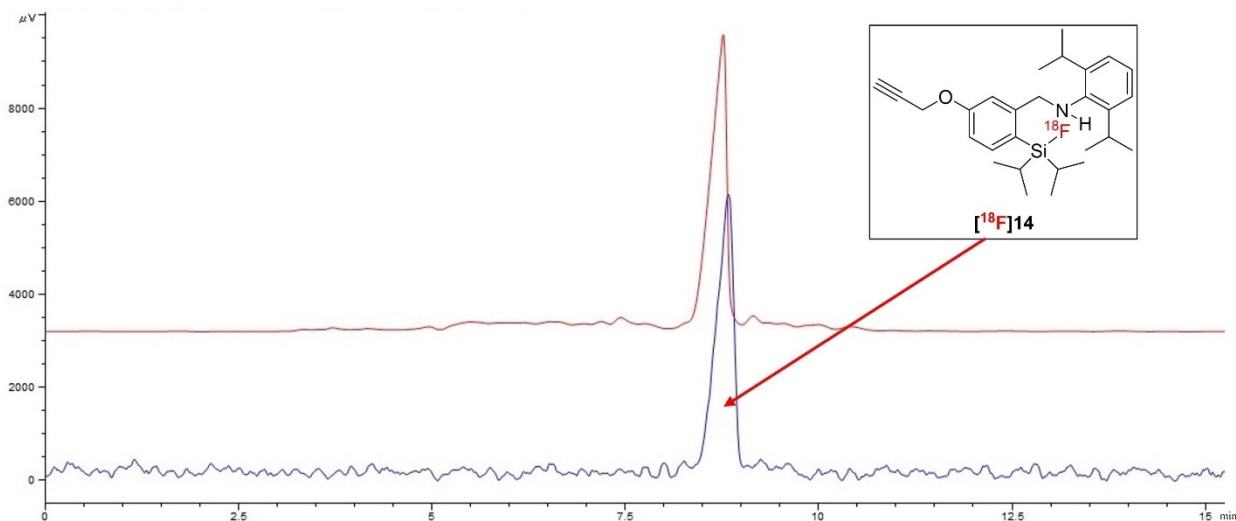


**Figure 1.** Crude reaction mixture of the formation of  $[^{18}\text{F}]\text{14}$ . The aliquot that was injected onto HPLC was spiked with a small amount of non-radioactive **14** to confirm the identity of the radioactive HPLC peak (blue line = radioactivity channel; red line = UV channel).

fluorination reactions based on nucleophilic [ $^{18}\text{F}$ ]F<sup>-</sup> anion labelling. Acetonitrile is an excellent dipolar aprotic solvent for  $^{18}\text{F}$ -radiofluorination and has proven its value in the development of the first-generation SiFA technology.

The [ $^{18}\text{F}$ ]F<sup>-</sup> was extracted from the aqueous solution obtained after the cyclotron bombardment of enriched [ $^{18}\text{O}$ ]water with protons, using a preconditioned potassium carbonate loaded quaternary methyl ammonium (hereafter referred to QMA) cartridge (46 mg K<sub>2</sub>CO<sub>3</sub>). The key to a successful *CycloSiFA* labelling in acetonitrile hinged on the sufficient acidification of the [ $^{18}\text{F}$ ]F<sup>-</sup> anion obtained from the QMA elution using tetraethyl ammonium tosylate (Et<sub>4</sub>NOTs) in acetonitrile containing a small amount of water.<sup>[41]</sup> To efficiently elute the [ $^{18}\text{F}$ ]F<sup>-</sup> from the QMA, Et<sub>4</sub>NOTs (10 mg, 33 nmol) was dissolved in a mixture of 300  $\mu\text{L}$  of water and 700  $\mu\text{L}$  of acetonitrile. Previously, we disclosed the “four-drop method” where more than 90 % of the [ $^{18}\text{F}$ ]F<sup>-</sup> radioactivity was eluted from the QMA cartridge within the first four drops.<sup>[21]</sup> Applied to our labelling scenario, this volume minimized eluate (ca. 150  $\mu\text{L}$ ) was azeotropically dried with acetonitrile to remove traces of water. An aliquot of the basic  $^{18}\text{F}$ -labelling cocktail was acidified using an optimized amount of oxalic acid and dissolved in acetonitrile to provide H[ $^{18}\text{F}$ ]F necessary for the *CycloSiFA* ring opening to proceed.

Two compounds were tested in this labelling scenario, compound **4** and the alkyne-derivatized precursor **13** (cf. Table 1, Scheme 5). The amount of oxalic acid had to be optimized for both reactions (cf. experimental part). Since the labelling reaction was performed at room temperature, the likelihood of H[ $^{18}\text{F}$ ]F evaporating from the reaction mixture was minimized. After a reaction time of 10 min at room temperature, an aliquot was taken and analysed using radio-TLC and radio-HPLC. Radiochemical conversion rates were found to be between 81  $\pm$  5 % and 90  $\pm$  5 % for **4** and **13**, respectively (Scheme 7). [ $^{18}\text{F}$ ]**14** was isolated for potential further prosthetic group Cu-catalysed click-radio-labelling using HPLC. The overall non-decay corrected radiochemical yield (RCY) was 46  $\pm$  4 % ( $n=3$ ) after HPLC purification (Figure 1).

Comparing the TLC results with the HPLC preparative yields revealed that some of the HPLC observed side products could not be identified via TLC. This explains the discrepancy between the RCC obtained from TLC readings and the preparative HPLC RCYs. Finally, the [ $^{18}\text{F}$ ]**14** was separated from the HPLC solvent by solid phase cartridge extraction. [ $^{18}\text{F}$ ]**14** and other *CycloSiFA* compounds currently in development will be used in future radiolabelling reactions.

## Conclusion

We have synthesized a variety of novel azasilole derivatives (five-membered rings) and proved their ability to undergo ring-opening by fluoride anion under mild and efficient conditions (low temperature, fast reaction, no by-product separation needed). Some of the azasiloles contain at the aryl backbone functional groups which are able to undergo

click-type chemistry allowing straightforward linkage to biomolecules on demand. This opens a new chapter of silicon-based  $^{18}\text{F}$  radiochemistry for PET tracer development fueled by SiFA's already perceptible clinical success. PET technology has been forecasted to see an enormous growth within the next decade. The concept holds potential to be extended to six-membered rings (for which ring-opening could proceed even faster and milder) and also to boron-based analogues. Especially tumour homing peptides (e.g. octreotide and octreotate) for diagnostic oncologic PET imaging could provide potential targets for *CycloSiFA* radiolabelling. We will further investigate whether our labelling conditions lead to a premature hydrolysis of the *CycloSiFA* precursor alongside the  $^{18}\text{F}$ -radiolabelling. By adding a silanol by-product to the reaction mixture, the effective  $A_m$  of the  $^{18}\text{F}$ -SiFA compound could be negatively affected. Obtaining higher molar activities in an optimized *CycloSiFA* labelling setup could provide an advantage over the currently used SiFA-based radiopharmaceuticals and consolidate its value as a new entry into  $^{18}\text{F}$ -labelling technologies.

## Acknowledgements

This work has been supported by the Natural Sciences and Engineering Research Council of Canada (NSERC), Discovery Grant to RS. The authors M.M., J.B., L.I., N.K., and K.J. are grateful to TU Dortmund for supporting this work. We thank the anonymous reviewers for valuable hints. Open Access funding enabled and organized by Projekt DEAL.

## Conflict of Interest

The authors declare no conflict of interest.

## Data Availability Statement

The data that support the findings of this study are available in the supplementary material of this article.

**Keywords:** Azasilole · Fluorine · Positron Emission Tomography · Ring Opening · Silicon

- [1] B. P. Burke, G. S. Clemente, S. J. Archibald, *Contrast Media Mol. Imaging* **2015**, *10*, 96–110.
- [2] a) R. Schirmacher, G. Bradtmöller, E. Schirmacher, O. Thews, J. Tillmanns, T. Siessmeier, H. G. Buchholz, P. Bartenstein, B. Wängler, C. M. Niemeyer, K. Jurkschat, *Angew. Chem. Int. Ed.* **2006**, *45*, 6047–6050; b) V. Bernard-Gauthier, M. L. Lepage, B. Waengler, J. J. Bailey, S. H. Liang, D. M. Perrin, N. Vasdev, R. Schirmacher, *J. Nucl. Med.* **2018**, *59*, 568–572; c) L. Gower-Fry, T. Kronemann, A. Dorian, Y. Pu, C. Jaworski, C. Wängler, P. Bartenstein, L. Beyer, S. Lindner, K. Jurkschat, B. Wängler, J. J. Bailey, R. Schirmacher, *Pharmaceuticals* **2021**, *14*, 701.

- [3] K. Chansaenpak, B. Vabre, F. P. Gabbaï, *Chem. Soc. Rev.* **2016**, *45*, 954–971.
- [4] S. J. Archibald, L. Allott, *EJNMMI Radiopharm. Chem.* **2021**, *6*, 30.
- [5] K. R. Scroggie, M. V. Perkins, J. M. Chalker, *Front. Chem.* **2021**, *9*, 687678.
- [6] Q. Zheng, H. Xu, H. Wang, W.-G. H. Du, N. Wang, H. Xiong, Y. Gu, L. Noodleman, K. B. Sharpless, G. Yang, P. Wu, *J. Am. Chem. Soc.* **2021**, *143*, 3753–3763.
- [7] J. J. Vaquero, P. Kinahan, *Annu. Rev. Biomed. Eng.* **2015**, *17*, 385–414.
- [8] S. C. Vaz, F. Oliveira, K. Herrmann, P. Veit-Haibach, *Br. J. Radiol.* **2020**, *93*, 20200095.
- [9] N. S. Goud, R. K. Joshi, R. D. Bharath, P. Kumar, *Eur. J. Med. Chem.* **2020**, *187*, 111979.
- [10] J. Ajenjo, G. Destro, B. Cornelissen, V. Gouverneur, *EJNMMI Radiopharm. Chem.* **2021**, *6*, 33.
- [11] R. Schirmacher, B. Wängler, J. Bailey, V. Bernard-Gauthier, E. Schirmacher, C. Wängler, *Semin. Nucl. Med.* **2017**, *47*, 474–492.
- [12] R. Ting, M. J. Adam, T. J. Ruth, D. M. Perrin, *J. Am. Chem. Soc.* **2005**, *127*, 13094–13095.
- [13] W. J. McBride, R. M. Sharkey, H. Karacay, C. A. D'Souza, E. A. Rossi, P. Laverman, C.-H. Chang, O. C. Boerman, D. M. Goldenberg, *J. Nucl. Med.* **2009**, *50*, 991–998.
- [14] N. Walter, J. Bertram, B. Drewes, V. Bahutski, M. Timmer, M. B. Schütz, F. Krämer, F. Neumaier, H. Endepols, B. Neumaier, B. D. Zlatopolskiy, *Eur. J. Med. Chem.* **2022**, *237*, 114383.
- [15] R. Bhalla, W. Levason, S. K. Luthra, G. McRobbie, G. Sander-son, G. Reid, *Chem. Eur. J.* **2015**, *21*, 4688–4694.
- [16] T. Long, N. Yang, M. Zhou, D. Chen, Y. Li, J. Li, Y. Tang, Z. Liu, Z. Li, S. Hu, *Clin. Nucl. Med.* **2019**, *44*, 452–458.
- [17] J. Lau, J. Pan, E. Rousseau, C. F. Uribe, S. R. Seelam, B. W. Sutherland, D. M. Perrin, K.-S. Lin, F. Bénard, *EJNMMI Res.* **2020**, *10*, 25.
- [18] G. Chausse, F. Benard, S. Harsini, J. Pan, H. Saprunoff, C. Uribe, H. Allan, D. Perrin, K.-S. Lin, D. Wilson, *J. Nucl. Med.* **2022**, *63*, 2270.
- [19] H. Ilhan, S. Lindner, S. Todica, C. C. Cyran, R. Tiling, C. J. Auernhammer, C. Spitzweg, S. Boeck, M. Unterrainer, F. J. Gildehaus, G. Böning, K. Jurkschat, C. Wängler, B. Wängler, R. Schirmacher, P. Bartenstein, *Eur. J. Nucl. Med. Mol. Imaging* **2020**, *47*, 870–880.
- [20] S. Lindner, C. Wängler, J. J. Bailey, K. Jurkschat, P. Bartenstein, B. Wängler, R. Schirmacher, *Nat. Protoc.* **2020**, *15*, 3827–3843.
- [21] J. J. Bailey, M. Wuest, M. Wagner, A. Bhardwaj, C. Wängler, B. Wängler, J. F. Valliant, R. Schirmacher, F. Wuest, *J. Med. Chem.* **2021**, *64*, 15671–15689.
- [22] a) W. Wan, N. Guo, D. Pan, C. Yu, Y. Weng, S. Luo, H. Ding, Y. Xu, L. Wang, L. Lang, Q. Xie, M. Yang, X. Chen, *J. Nucl. Med.* **2013**, *54*, 691–698; b) M. Unterrainer, S. C. Kunte, L. M. Unterrainer, A. Holzgreve, A. Delker, S. Lindner, L. Beyer, M. Brendel, W. G. Kunz, M. Winkelmann, C. C. Cyran, J. Ricke, K. Jurkschat, C. Wängler, B. Wängler, R. Schirmacher, C. Belka, M. Niyazi, J.-C. Tonn, P. Bartenstein, N. L. Albert, *Eur. J. Nucl. Med. Mol. Imaging* **2023**, *50*, 3390–3399.
- [23] M. Novák, L. Dostál, M. Alonso, F. De Proft, A. Růžicka, A. Lyčka, R. Jambor, *Chem. Eur. J.* **2014**, *20*, 2542–2550.
- [24] a) A. Höhne, L. Yu, L. Mu, M. Reiher, U. Voigtmann, U. Klar, K. Graham, P. A. Schubiger, S. M. Ametamey, *Chem. Eur. J.* **2009**, *15*, 3736–3743; b) Preliminary studies on *CycloSiFA* revealed a comparable stability against hydrolysis ( $t_{1/2, \text{CycloSiFA}} = 286$  h compared to  $t_{1/2, \text{Ametamey}} = 302$  h).
- [25] a) Q. Li, M. Driess, J. F. Hartwig, *Angew. Chem. Int. Ed.* **2014**, *53*, 8471–8474; *Angew. Chem.* **2014**, *126*, 8611–8614; b) Deposition numbers 2265385 (for **4**) and 2265386 (for **10**) contain the supplementary crystallographic data for this paper. These data are provided free of charge by the joint Cambridge Crystallographic Data Centre and Fachinformationszentrum Karlsruhe Access Structures service.
- [26] Derivatives with Mesityl substituents are depicted in the Supporting Information. Ph, *t*Bu, *i*Pr and Me-derivatives were successfully substituted with chlorosilanes, but the imines decomposed during workup to substituted benzaldehyde and amine.
- [27] S. Laue, L. Greiner, J. Wöltinger, A. Liese, *Adv. Synth. Catal.* **2001**, *343*, 711–720.
- [28] a) H. Gillier-Pandraud, *Bull. Soc. Chim. Fr.* **1967**, *6*, 1988–1995; b) V. E. Zavodnik, V. K. Bel'skii, P. M. Zorkii, *J. Struct. Chem.* **1988**, *28*, 793–795; c) C. Scheringer, *Z. Kristallogr.* **1963**, *119*, 273–283; d) D. R. Allan, S. J. Clark, A. Dawson, P. A. McGregor, S. Parsons, *Acta Crystallogr. Sect. B* **2002**, *58*, 1018–1024.
- [29] a) M. Mantina, A. C. Chamberlin, R. Valero, C. J. Cramer, D. G. Truhlar, *J. Phys. Chem. A* **2009**, *113*, 5806–5812; b) F. Feige, L. A. Malaspina, F. Kleemiss, J. F. Kögel, S. Ketkov, E. Hupf, S. Grabowsky, J. Beckmann, *Dalton Trans.* **2023**, *52*, 5918–5925.
- [30] a) H. Sak, M. Mawick, N. Krause, *ChemCatChem* **2019**, *11*, 5821–5829; b) T. R. Chan, R. Hilgraf, K. B. Sharpless, V. V. Fokin, *Org. Lett.* **2004**, *6*, 2853–2855.
- [31] M. Kazayuki, H. Chuji, N. Fumio (Univ Chiba), JP2015224231 A, **2015**.
- [32] The Supporting Information contains details concerning the byproducts. Different TBS-substituted byproducts can be deprotected and recycled.
- [33] N. Savisto, J. Bergman, J. Aromaa, S. Forsback, O. Eskola, T. Viljanen, J. Rajander, S. Johansson, J. Grigg, S. Luthra, O. Solin, *Nucl. Med. Biol.* **2018**, *64–65*, 8–15.
- [34] F. Fächter, S. Preusche, P. Mäding, J. Zessin, J. Steinbach, *Nuklearmedizin* **2008**, *47*, 116–119.
- [35] J. Bergman, O. Eskola, P. Lehtikoinen, O. Solin, *Appl. Radiat. Isot.* **2001**, *54*, 927–933.
- [36] M. S. Berridge, S. M. Apana, J. M. Hersh, *J. Labelled Compd. Radiopharm.* **2009**, *52*, 543–548.
- [37] C. S. Dence, T. J. McCarthy, M. J. Welch, Ionic contaminants (radioactive and nonradioactive) in irradiated [O-18] water. Preliminary results of a comparative study. *Proceedings of the sixth workshop on Targetry and target chemistry*, **1995**, 199–205, <http://wtcc.triumf.ca/pdf/1995/Sec5-7.pdf>, Accessed date: 3 December 2017.
- [38] M. R. Kilbourn, J. T. Hood, M. J. Welch, *Int. J. Appl. Radiat. Isot.* **1984**, *35*, 599–602.
- [39] M. R. Kilbourn, P. A. Jerabek, M. J. Welch, *Int. J. Appl. Radiat. Isot.* **1985**, *36*, 327–328.
- [40] O. Solin, J. Bergman, M. Haaparanta, A. Reissell, *Appl. Radiat. Isot.* **1988**, *39*, 1065–1071.
- [41] J. A. H. Inkster, V. Akurathi, A. W. Sromek, Y. Chen, J. L. Neumeyer, A. B. Packard, *Sci. Rep.* **2020**, *10*, 6818.

Manuscript received: June 26, 2023

Accepted manuscript online: October 18, 2023

Version of record online: November 10, 2023